Adaptive Capacity Planning Formulation for Infrastructure Networks

Nazanin Morshedlou[1]; Kash Barker[2]; Charles D. Nicholson[3]; and Giovanni Sansavini[4]

Abstract: This research investigates the adaptive capacity enhancement problem of network systems and proposes a framework for allocating limited resources during the response phase in the aftermath of a disruptive event. The proposed formulation optimizes the performance level to which a network can quickly and temporarily adapt to after a disruption. Optimal resource allocation is determined with respect to the spatial dimensions of network components and available resources, the effectiveness of the resources, the importance of each element, and the system-wide impact to potential flows within the network. The proposed framework is amenable for use with a variety of component importance measures (IM) that exist in literature as well as various settings of priorities for demand nodes and time periods. These importance measures and priorities, and the specifics of the disruptive event, may result in vastly different resource allocation strategies. The efficacy of the optimization model is demonstrated on a case study based on a French electric power transmission network under simulated disruptions. Multiple component importance metrics and resource availability scenarios are examined. **DOI: 10.1061/(ASCE)IS.1943-555X.0000432.**

Author keywords: Adaptive capacity; Criticality; Accessibility; Connectivity; Importance measures.

Introduction and Motivation

The US government has increasingly emphasized resilience planning for the country's critical infrastructure systems. Presidential Policy Directive 21 (White House 2013) states that critical infrastructure "must be secure and able to withstand and rapidly recover from all hazards," where the combination of "withstanding" and "recovering" from disruptions constitutes *resilience*. The resilient operation of critical infrastructures is "essential to the Nation's security, public health and safety, economic vitality, and way of life" (DHS 2013). DHS planning documents highlight terrorist attacks, natural disasters, and man-made hazards, all of which could exacerbate aging US infrastructure systems, particularly transportation infrastructure (e.g., roads, bridges, waterway facilities), whose state of repair has been given a grade of D+ (ASCE 2017) for several years.

Definitions, models, and measures of resilience pervade the literature (Hosseini et al. 2016), across the social sciences (Magis 2010; Sullivan et al. 2010; Aldrich 2012; Cutter et al. 2014), engineering (Reed et al. 2009; Cimellaro et al. 2010; Ouyang and Duenas-Osorio 2012; Francis and Bekera 2014; Nan and Sansavini 2017), and risk contexts (Haimes 2009; Aven 2011), to name just a few. Fig. 1 offers a paradigm for the performance of a system before, during, and after a disruption (Henry and Ramirez-Marquez 2012; Barker et al. 2013; Pant et al. 2014), where performance over time is measured generally with $\varphi(t)$ (e.g., traffic flow along a railway network). Highlighted in Fig. 1 are two primary dimensions of resilience: (1) vulnerability, or the lack of ability of a system to withstand a disruption and maintain its performance level, and (2) recoverability, or the ability of a system to improve and recover system performance in a timely manner. This work focuses on the vulnerability dimension of resilience, particularly as it applies to networks. The adverse impact that a disruption has on network performance is a function of the network's vulnerability (Newman 2005; Zio et al. 2008; Jonsson et al. 2008; Zhang et al. 2011).

Vugrin and Camphouse (2011) define the *resilience capacity* of a system as a function of its absorptive, adaptive, and restorative capacities. Naturally, *absorptive capacity* deals with the extent to which a system is able to absorb shocks from disruptive events and prevent collapse, implying that pre-disruption planning can increase absorptive capacity. An example of building absorptive capacity is strengthening the bridges with continuous spans during construction, or reconstruction, in the Northridge area of San Fernando Valley in Los Angeles (Cooper et al. 1994). *Adaptive capacity* is the extent to which a system can quickly adapt after a disruption by temporary means. Examples of adaptive capacity include emergency debris removal from transportation routes and temporary reconstitution of emergency services (Bye 2013). In this paper, focus is given to technical strategies to enhance adaptive capacity; alternative mitigation strategies, such as behavioral modifications (e.g., employees working from home to reduce traffic on damaged roads), are not investigated. Finally, the *restorative capacity* of a system is the extent to which it can recover from a disruption in a more long-term manner, for example, the reconstruction of destroyed infrastructure. As such, absorptive, adaptive, and restorative capacities can be viewed as first, second, and third lines of

[1]Ph.D. Candidate, School of Industrial and Systems Engineering, Univ. of Oklahoma, 202W. Boyd St., Room 124, Norman, OK 73019. Email: nazanin.morshedlou@ou.edu

[2]Associate Professor, Anadarko Presidential Professor, School of Industrial and Systems Engineering, Univ. of Oklahoma, 202W. Boyd St., Room 124, Norman, OK 73019 (corresponding author). Email: kashbarker@ou.edu

[3]Assistant Professor, School of Industrial and Systems Engineering, Univ. of Oklahoma, 202W. Boyd St., Room 124, Norman, OK 73019. Email: cnicholson@ou.edu

[4]Assistant Professor, Dept. of Mechanical and Process Engineering, Institute of Energy Technology, ETH-Zürich, Rämistrasse 101, 8092 Zürich, Switzerland. Email: sansavig@ethz.ch

Note. This manuscript was submitted on January 26, 2017; approved on March 9, 2018; published online on July 23, 2018. Discussion period open until December 23, 2018; separate discussions must be submitted for individual papers. This paper is part of the ***Journal of Infrastructure Systems***, © ASCE, ISSN 1076-0342.

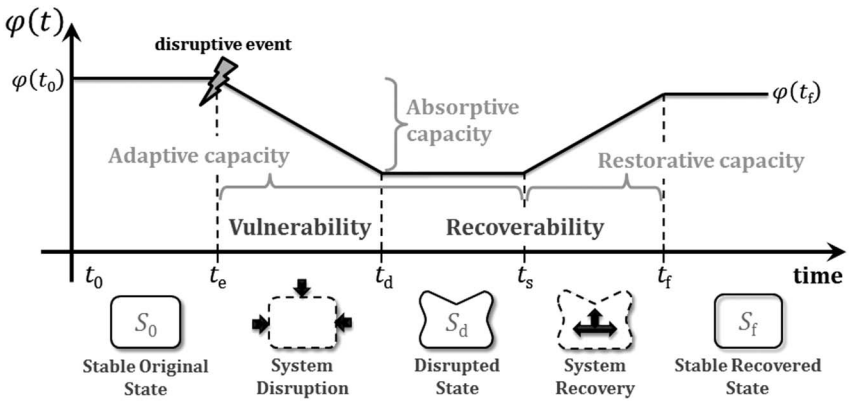

Fig. 1. System performance across system states.

defense, respectively (Hosseini and Barker 2016). Relative to Fig. 1, absorptive and adaptive capacities address a system's vulnerability, where a system's recoverability is a function of its restorative capacity.

Resources engaged after a disruption encompass roadside debris removal equipment (Aksu and Ozdamar 2014; Çelik et al. 2015), construction crews (Averbakh 2012), repair crews (Duque et al. 2016), and emergency response (Jacobson et al. 2012). Particularly for electric power networks, such resources have included temporary equipment to replace disabled high voltage transformers (Salmeron and Wood 2015), crews removing fallen objects causing shorted circuits (Wei et al. 2016), and inserting backup power (e.g., generators) in the system (Division of Emergency Management 2008). The assignment of and scheduling of these resources to disrupted network components is important (Duque et al. 2016; Arab et al. 2015; Aksu and Ozdamar 2014), though not many have studied such a spatially-located resource allocation in an adaptive or restorative capacity context (Akbari and Salman 2017; Görmez et al. 2011; Kasaei and Salman 2016). By considering the worst disruption scenario that may affect the network, we plan to allocate and schedule resources to increase the adaptive capacity of the network immediately after disruption and, consequently, expedite the long-term recovery.

This work provides a mixed integer linear programming (MILP) formulation to allocate spatially located resources to improve a network's adaptive capacity. Three characteristics are integrated into the formulation: (1) link criticality, or the importance of a link in enabling the performance of the network; (2) network accessibility, or the extent to which capacity is degraded across links in the network; and (3) network connectivity, or the extent to which demand is being met at demand nodes. After a disruptive event, the limited, spatially distributed resources are allocated to network components to quickly engage the affected components by proportionally improving their functionality. While these resources have potentially only limited effectiveness, their optimal allocation can significantly reduce vulnerability of the larger system in the immediate term.

The organization of this paper is as follows. First, various techniques for modeling absorptive, adaptive, and restorative capacity are reviewed. Second, the optimization formulation is proposed for integrating component criticality, accessibility, and connectivity. Next, the optimization formulation is applied to several network instances motivated by the 400 kV French electric power transmission network. Finally, conclusions, limitations, and directions for future work are provided.

Methodological Background

There are two primary research streams related to the management of network disruptions: (1) vulnerability measurement and reduction; and (2) recovery optimization.

Most work in measuring and reducing vulnerability addresses *absorptive capacity*, or mitigation efforts to identify and fortify nodes in advance of a disruption. Many techniques have been developed to measure network vulnerability and identify the important network components contributing to vulnerability. Cohen et al. (2000) introduce a criterion based on percolation theory to identify critical nodes, the absence of which lead to disconnections in the network. Vromans et al. (2006) examine the vulnerability of a railway network to reduce the interdependencies between trains after a disruption. Jenelius et al. (2006) introduces link importance and site exposure indices which are divided into two groups: (1) an equal opportunity perspective where all roads are equally important; and (2) a social efficiency perspective where more frequently used roads are considered more important.

One of the primary reasons to measure vulnerability is to understand the extent to which a disruptive event affects network performance to prepare the network for potential consequences. Instead of single link or node disruption, Jenelius and Mattsson (2012) adopt grids of uniformly shaped and sized cells, where each cell represents the extent of an event disrupting any intersecting links. Unlike single link failures, where the link flow and the redundancy in the surrounding network determine the impacts, the vulnerability to spatially spread events shows a markedly different geographical distribution. Jenelius and Mattsson (2015) perform regional vulnerability analyses in large-scale road networks due to both single link closures and area-covering disruptions.

Lempert and Groves (2010) focus on *adaptive capacity*, implementing robust decision-making approaches to plan adaptive strategies against catastrophic events. Using a simulation-based approach, they identify the different sets of vulnerable network components that adversely impact network performance from various perspectives. Francis and Bekera (2014) propose a resilience framework to focus on the achievement of adaptive capacity along with absorptive and restorative capacity enhancement. They quantify adaptive capacity as the proportion of original system performance retained after the new stable level of performance in the aftermath of disruption. Particularly in power grid networks, Ghasemi and Parniani (2016) propose an adaptive control algorithm to prevent the overvoltage that may happen in the network immediately after disruptions. Arghandeh et al. (2016) demonstrate some adaptive capacity enhancement activities in the physical structure of power

grid networks (e.g., reinforcing towers and poles), increasing the flexibility of the network by installing temporary means (e.g., transformers and sensors) and prioritizing components with fortification. Fang and Sansavini (2017) co-optimize power grid expansion and installation of line switching devices to mitigate the supply disservice in the aftermath of disruptions and enhance resilience by system hardening and re-configurability. In transportation networks, Zhang et al. (2015) consider the topological and spatial form of transportation networks and their impact on the flexibility of the network to adapt to disruption during response. They investigate the role of topological attributes of a transportation network (e.g., grid, hub-and-spoke, scale-free, and small-world) in its ability to cope with disruptions by temporary means or redirecting routes to decrease network performance. El-Rashidy and Grant-Muller (2014) propose an integrated method including exhaustive optimization and fuzzy logic, combining different vulnerability measures (traffic flow, capacity, length, flow, and free flow) to introduce a unique index to increase the adaptive capacity of the transportation networks after disruptions.

Work in recoverability optimization focusing on *restorative capacity* is a burgeoning area of research. Nurre et al. (2012) develop an integrated network design and scheduling model to restore networks following an extreme disruptive event, determining restoration efforts by selecting a set of links that optimized residual paths. Similarly, Nurre and Sharkey (2014) develop network design and scheduling model to minimize the amount of time required to reach a certain level of network performance. Averbakh (2012) and Averbakh and Pereira (2012) consider the problem of scheduling the restoration of a transportation network with fixed restoration rate service units, minimizing restoration time. Several other works have recently addressed inspection and repair optimization in electric power networks (Xu et al. 2007; Arab et al. 2015, 2016).

As opposed to *absorptive capacity* (emphasizing decisions during $t \in (t_0, t_e]$ from Fig. 1) and *restorative capacity* (emphasizing decisions during $t \in (t_d, t_f]$), work proposed here addresses the short-term allocation of resources after a disruption to improve *adaptive capacity* during $t \in (t_e, t_d]$. The allocation of resources during this timeframe has little treatment in the literature [e.g., developing short-term routes after a disruption (MacKenzie et al. 2012; Chen et al. 2014)].

Problem Formulation

Consider a directed network $G = (N, A)$, where N is the set of nodes and $A \subseteq N \times N$ is the set links. There is a set of supply nodes $N_+ \subseteq N$, a set of demand nodes $N_- \subseteq N$, and a set of transition nodes $N_= \subseteq N$. Each supply node $i \in N_+$ can supply amount o_i in each time period, and each demand node $i \in N_-$ demands amount b_i in each time period.

Each link $(i, j) \in A$ has a defined predisaster capacity u_{ijt_e} and a precalculated flow value based on the summation of flow values across supply and demand nodes before the disruptive event that occurs at time t_e in Fig. 1. Without loss of generality, *components* in the context of this research refer to links, as any node failure can be represented by an appropriate set of link failures.

Let $A' \subseteq A$ denote the set of links in the network that are impacted by a disruptive event at time t_e. A link disruption is modeled by a reduction in link capacity. A reduction to a capacity level of 0 represents a total loss of the link. There exists a set of adaptive capacity resources that can be allocated promptly after a disruptive event to begin immediate-term recovery of system functionality. Each resource can send a specific number of services to disrupted links. Each service may have a specific processing time and complete its task in any time period $t \in \{1, \ldots, T\}$, and the first time period starts from t_e, immediately after the occurrence of a disruptive event, and the last time period, T, ends at t_d, when short-term response ends. We define R resource types. Each has a service capacity M^r denoting the number of available resources of type $r \in \{1, \ldots, R\}$ and has a number of services U^r that can be performed by resource type $r \in \{1, \ldots, R\}$. In electric power networks, each of these resources might refer to a set of work crews that temporarily (1) harden distribution links; or (2) reinforce towers and poles to prevent cascading effects and overvoltage disruptions. The capability of each set of work crews to fortify a disrupted link depends on, for example, the experience of the technicians and the quality of their equipment. Network components are located in a set of spatial clusters $s \in \{1, \ldots, S\}$ that aid in the assignment of these resources, and the resources allocated to cluster s can only serve the disrupted components in that cluster. It is assumed that there are limited available resources that can be allocated to minimize the adverse effects of a disruption in the first few time periods after a disruptive event. These resources temporarily support the damaged network and alleviate the severity of the adverse effects on the components. Furthermore, resources allocated to reduce vulnerability may more effectively reduce the subsequent longer-term time and costs of recovery.

The three primary components of the optimization problem proposed here for assigning adaptive capacity resources are: (1) criticality; (2) accessibility; and (3) connectivity. For criticality, the importance of each component is measured such that more important network components are prioritized to increase adaptive capacity in the minimum possible time horizon. For accessibility, the effects of the disruption on component capacity is measured and emphasized. For connectivity, unmet demand for critical demand nodes is addressed. Previous work (Ouyang et al. 2012; Nurre et al. 2012; Demirel et al. 2015) explores the relationship between connectivity and accessibility; this work includes the role of criticality, and its relationship to connectivity and accessibility, during short-term response.

Criticality

The *criticality* of network component $(i, j) \in A'$ is primarily a function of its importance in the network. The importance of a component, measured on [0,1] with values close to 1 suggesting greater importance, can be measured from multiple perspectives. Several authors have proposed importance measures based on the connectivity of the network when the component is removed, among other graph-theoretic measures (Holme et al. 2002; Albert et al. 2004; Holmgren 2006; Johansson and Hassel 2010; Johansson et al. 2011; Wang et al. 2013). Several authors have explored measures that quantify the importance of components to flow along the network (Nagurney and Qiang 2007a, b, 2008; Rocco et al. 2010; Nicholson et al. 2016).

Each network component has a certain importance measure value, where I_{ij}^{π} is the importance measure calculated for $(i, j) \in A$ of type π, where the πth importance measure represents one of many differing perspectives on importance [e.g., maximum flow count, edge centrality, and edge flow importance measures (Nicholson et al. 2016)]. The use of I_{ij}^{π} in Eq. (1) is to aid in understanding component criticality prior to the actual allocation of resources to the clusters. Values of I_{ij}^{π} closer to 1 would rank link (i, j) as more critical in terms of receiving adaptive capacity services sent from the allocated resource. The criticality coefficient is captured in the objective function with Eq. (1), where y_{ijt}^{rs} is a binary variable equal to 1 when the processing time, p^r, for

resource $r \in \{1, \ldots, R\}$ to service link (i, j) in cluster $s \in \{1, \ldots, S\}$ is completed at time period t and 0, otherwise

$$I_{ij}^{\pi} y_{ijt}^{rs} \tag{1}$$

In this paper, we focus on links that are important to the aggregate flow delivered to all demand nodes, and use three (pre-disruption) flow-based importance measures proposed by Nicholson et al. (2016): (1) *max flow edge count*, $I_{MFcount} = [1/n(n-1)]\sum_{\bar{s},\bar{t}\in V}\mu_{\bar{s}\bar{t}}(i,j)$, where $\mu_{\bar{s}\bar{t}}(i,j)$ is a binary parameter and equals 1 if link (i, j) is used in a given source-sink max flow path; (2) *edge flow centrality*, $I_{Flow} = [\sum_{\bar{s},\bar{t}\in V}\omega_{\bar{s}\bar{t}}(i,j)/\sum_{\bar{s},\bar{t}\in V}\omega_{\bar{s}\bar{t}}]$, where $\omega_{\bar{s}\bar{t}}(i,j)$ is the flow on link (i, j) for all possible source-sink paths and $\omega_{\bar{s}\bar{t}}$ is the maximum feasible flow from source $\bar{s}$ to sink $\bar{t}$ for any source-sink path $\bar{s}$, $\bar{t} \in V$; and (3) *flow capacity rate*, $I_{FCR} = [1/n(n-1)][\sum_{\bar{s},\bar{t}\in V}\omega_{\bar{s}\bar{t}}(i,j)/c_{ij}]$, where c_{ij} is the capacity of link (i, j).

Accessibility

Morris et al. (1979) introduce accessibility as the ease whereby flow can reach from one location to another. In vulnerability analyses, both single component and area-covering failures have been studied (Berdica and Mattsson 2007; Jenelius and Mattson 2012). However, focusing on single component failure or a location failure may not be an appropriate method in origin/destination or supply/demand problems due to the nature of such networks. Instead of considering the accessibility of single components or a certain area, this paper maximizes the accessibility of the entire network by adding adaptive capacity to disrupted links. The accessibility of link $(i, j) \in A'$ prior to the occurrence of a disruptive event is measured by its predisaster capacity

$$V_{ijt_e} = u_{ijt_e} \tag{2}$$

Shown in Eq. (3) is the comparison of (1) the network operating under the post-disruption performance (its performance after the disruptive event without taking any response or recovery action); and (2) its enhanced performance with the implementation of the adaptive capacity resource assignment strategy. First, the change in the capacity of components and subsequent network degradation are calculated. Second, as the network components are spatially clustered with adaptive capacity resources located in those clusters, resources are dispatched to temporarily adapt the network to maintain its baseline performance level.

Eq. (3) defines V_{ijt}, the accessibility measure for link $(i, j) \in A'$ after disruption. In this paper, V_{ijt} can be interpreted as the capacity of a disrupted link (i, j) after its fortification process is completed. Baseline network performance (its performance before the disruptive event) is measured immediately prior to t_e as depicted in Fig. 1. The fully disrupted network performance is measured at time $t \in \{1, \ldots, T\}$. As such, u_{ijt_e} is the capacity on link (i, j) before the disruptive event, and u_{ijt_d} is the capacity of link (i, j) at time t_d.

The amount of performance degradation for link (i, j) in each time period t is mitigated by the factor $H_{ij}^{r}\sum_{c=1}^{t} y_{ijc}^{rs}$, where $0 \le H_{ij}^{r} \le 1$ measures the extent to which the assignment of resource $r \in \{1, \ldots, R\}$ to component (i, j) increases accessibility and $\sum_{c=1}^{t} y_{ijc}^{rs}$ is 1 if the processing time of component (i, j) in cluster s is completed in the time period c, $c \in \{1, \ldots, t\}$, by resource r

$$V_{ijt} = u_{ijt_d} + \left(\sum_{r=1}^{R}\sum_{s=1}^{S} H_{ij}^{r}\sum_{c=1}^{t} y_{ijc}^{rs}\right)(u_{ijt_e} - u_{ijt_d}) \tag{3}$$

Connectivity

Connectivity is a graph theoretic measure of the structure of a network (Demirel et al. 2015). Studies on connectivity enhancement are performed with a broad range of connectivity measures such as diameter, number of cycles, cost, detour index, pi index, eta index, theta index, and average nearest neighbors' degree (Hansen 1959; Waters 2006; Jenelius et al. 2006; Erath et al. 2009; Rodrigue et al. 2013; TDM 2013; Sullivan et al. 2010; Demirel et al. 2015). In origin/destination problems, enhanced connectivity leads to less unsatisfied demand when the network is disrupted.

In this work, the connectivity of a disrupted network is enhanced by reducing the difference between baseline and disrupted *aggregate* flows, or the total amount of flow that arrives to the demand nodes (Nurre et al. 2012). This is calculated in Eq. (4), where φ_{it_e} is a parameter representing the aggregate flows reaching demand node i prior to a disruptive event at time t_e, and φ_{it} is a variable that quantifies the aggregate flows reaching to demand node $i \in N_{-}$ during $t \in \{1, \ldots, T\}$. So that Eq. (4) represents a proportional value that is commensurate with other terms in the subsequent objective function, φ_{it_e} is included in the denominator

$$\mu_t w_i \frac{(\varphi_{it_e} - \varphi_{it})}{\varphi_{it_e}} \tag{4}$$

The parameter w_i is an importance weight assigned to demand node i. Such an importance weight could be calculated from a graph theory measure (e.g., centrality), by an economic index (e.g., economic potential), or some other decision-maker-driven value (e.g., a hospital may have a higher priority than a residential location) (Demirel et al. 2015; Nurre et al. 2012). In this paper, each demand node is assigned a weight based on its priority, and the demand node within more populated areas is considered a higher priority relative to other demand nodes. The parameter μ_t is the weight associated with the performance of the network in each time period t.

Model Formulation

The objective function and constraints considered in this work represent the integration of criticality, accessibility, and connectivity, with the goal being to assign spatial resources to improve the adaptive capacity of a network after a disruption.

The variables in the model formulation are divided into three categories: (1) network flow variables; (2) resource allocation variables; and (3) resource assignment variables. For $(i, j) \in A'$ and for $t \in \{1, \ldots, T\}$, x_{ijt} is the network flow variable on link (i, j) at time t, and φ_{it} is a continuous variable for each demand node $i \in N_{-}$, representing the amount of demand that is met at time t. The resource allocation variable is binary variable z^{rs} for $r \in \{1, \ldots, R\}$ and $s \in \{1, \ldots, S\}$, which indicates resource r is allocated to spatial cluster s. The resource assignment variable y_{ijt}^{rs} is a binary variable for $(i, j) \in A'$, $s \in \{1, \ldots, S\}$, $r \in \{1, \ldots, R\}$ that represents that link (i, j) from spatial cluster s is serviced by resource r. The sets, parameters, and variables used in the following problem formulation are found in the Notation list at the end of the paper.

The objective function for the short-term adaptive capacity resource allocation problem in Eq. (5) minimizes (1) the disruptive impacts to the more critical components with $\sum_{(i,j)\in A'}\sum_{r=1}^{R}\sum_{s=1}^{S}\sum_{t=1}^{T} -I_{ij}^{\pi} y_{ijt}^{rs}$ (criticality); and (2) the unsatisfied demand with $\sum_{i\in N_{-}}\sum_{t=1}^{T}\mu_t w_i[(\varphi_{it_e} - \varphi_{it})/\varphi_{it_e}]$ (connectivity). Accessibility is addressed by Eq. (11). Furthermore, a weighting factor could be added to each of these terms to

model tradeoffs between component criticality and unsatisfied demand

$$\min \sum_{(i,j)\in A'} \sum_{r=1}^{R} \sum_{s=1}^{S} \sum_{t=1}^{T} - I_{ij}^{\pi} y_{ijt}^{rs} + \sum_{i\in N_-} \sum_{t=1}^{T} \mu_t w_i \frac{(\varphi_{it_e} - \varphi_{it})}{\varphi_{it_e}} \quad (5)$$

$$\sum_{j:(i,j)\in A} x_{ijt} - \sum_{j:(j,i)\in A} x_{jit} \le o_i \quad \forall\, i \in N_+, \quad \forall\, t \in \{1, \ldots, T\} \quad (6)$$

$$\sum_{(i,j)\in A} x_{ijt} - \sum_{(j,i)\in A} x_{jit} = 0 \quad \forall\, i \in N_=, \quad \forall\, t \in \{1, \ldots, T\} \quad (7)$$

$$\sum_{(i,j)\in A} x_{ijt} - \sum_{(j,i)\in A} x_{jit} = -\varphi_{it} \quad \forall\, i \in N_-, \quad \forall\, t \in \{1, \ldots, T\} \quad (8)$$

$$0 \le \varphi_{it} \le b_i \quad \forall\, i \in N_-, \quad \forall\, t \in \{1, \ldots, T\} \quad (9)$$

$$0 \le x_{ijt} \le u_{ijt_e} \quad \forall\, (i,j) \in A/A', \quad \forall\, t \in \{1, \ldots, T\} \quad (10)$$

$$0 \le x_{ijt} \le V_{ijt} \quad \forall\, (i,j) \in A', \quad \forall\, t \in \{1, \ldots, T\} \quad (11)$$

$$\sum_{s=1}^{S} z^{rs} \le M^r \quad \forall\, r \in \{1, \ldots, R\} \quad (12)$$

$$\sum_{r=1}^{R} z^{rs} \le 1 \quad \forall\, s \in \{1, \ldots, S\} \quad (13)$$

$$\sum_{t=1}^{T} \sum_{(i,j)\in A'} \left(1 + \left\lfloor \frac{t - (l - p^r + 1)}{T} \right\rfloor\right) y_{ijt}^{rs} \le U^r z_{rs}$$
$$\forall\, s \in \{1, \ldots, S\}, \quad \forall\, r \in \{1, \ldots, R\} \quad (14)$$

$$\sum_{s=1}^{S} \sum_{r=1}^{R} \sum_{t=1}^{T} y_{ijl}^{rs} \le 1 \quad \forall\, (i,j) \in A' \quad (15)$$

$$y_{ijt}^{rs} \le \theta_{ij}^{s} \quad \forall\, (i,j) \in A',$$
$$\forall\, r \in \{1, \ldots, R\}, \quad \forall\, s \in \{1, \ldots, S\}, \quad \forall\, t \in \{1, \ldots, T\} \quad (16)$$

$$\sum_{t=1}^{p^r - 1} y_{ijt}^{rs} = 0 \quad \forall\, (i,j) \in A',$$
$$\forall\, r \in \{1, \ldots, R\}, \quad \forall\, s \in \{1, \ldots, S\} \quad (17)$$

$$z^{rs} \in \{0, 1\} \quad \forall\, r \in \{1, \ldots, R\}, \quad \forall\, s \in \{1, \ldots, S\} \quad (18)$$

$$y_{ijt}^{rs} \in \{0, 1\} \quad \forall\, r \in \{1, \ldots, R\},$$
$$\forall\, s \in \{1, \ldots, S\}, \quad \forall\, (i,j) \in A, \quad \forall\, t \in \{1, \ldots, T\} \quad (19)$$

$$x_{ijt} \ge 0 \quad \forall\, (i,j) \in A, \quad \forall\, t \in \{1, \ldots, T\} \quad (20)$$

$$\varphi_{it} \ge 0 \quad \forall\, i \in N_-, \quad \forall\, t \in \{1, \ldots, T\} \quad (21)$$

Eqs. (6)–(8) are network flow constraints over all available links in the network in time period t. According to Fig. 1, a disruptive event occurs at time period t_e, and the network performance decreases until it reaches its minimum performance at time t_d. Eq. (6) ensures that flow generated from supply nodes does not exceed their supply o_i, $i \in N_+$. Eq. (7) ensures that no flow is generated from or delivered to transmission nodes. Eq. (8) delivers the amount of flow that satisfies demand nodes while not exceeding their demands b_i, $i \in N_-$ in Eq. (9). The flow of an available link does not exceed its capacities, as ensured by Eqs. (10) and (11). In Eqs. (12) and (13), z^{rs} is a binary variable that equals 1 when resource $r \in \{1, \ldots, R\}$ is allocated in cluster $s \in \{1, \ldots, S\}$ and 0 otherwise. These two constraints ensure that the number of allocated resources does not exceed the number of available resources, M^r, and only one resource is allowed to be allocated to each cluster, respectively. Each allocated resource in each cluster assigns a specific number of services to the most critical disrupted components in that cluster. For each cluster, Eq. (14) ensures that the number of disrupted components being fortified by the allocated resource in each time period does not exceed its service capacity. It is assumed that a resource cannot strengthen adaptive capacity unless it is allocated to a cluster, and when it is allocated to a cluster, it is a candidate for being assigned to a disrupted component. Eq. (15) ensures that each disrupted link is scheduled at most to one service sent from the allocated resource. Eq. (16) ensures that an allocated resource to a cluster is only allowed to service the disrupted links in that cluster. Eq. (17) is a logical constraint that ensures that strengthening adaptive capacity cannot be performed earlier than the required processing time, p^r, or the time required for any service sent by resource $r \in \{1, \ldots, R\}$ to a disrupted link. Finally, Eqs. (18)–(21) describe the nature of the decision variables.

Case Study: 400-kV French Power Transmission

The proposed formulation is exemplified with reference to a power transmission network in France, extracted from topological data for the 400-kV transmission lines of RTE (2013). According to the detailed description extracted from RTE (2013), this network is an undirected graph with 171 substations (nodes) and 220 transmission lines (links) summing up to more than 28,387 km. There are 26 generators which generate power and 145 distributers which receive power. Some of the generators and distributers also transmit power from other generators to distributers. From a topological perspective, the weights of the links, which are assumed as their capacity, is identical. However, from a resilience point of view, each link is assigned a level of criticality. Following Fang et al. (2014), only power plants with installed capacities more than 1,000 MW are considered.

A modified version of the disrupted French transmission network was produced by integrating the approaches of Alipour et al. (2014) and Fang et al. (2014). The transmission network is depicted in Fig. 2, which shows the relationships among pairs of nodes, the number of links, and the spatial location of substation nodes. The capacity of each transmission line in the undirected network is 6,000 MW, and the total network flow and aggregate flow for undisrupted network are 306,253 and 84,988 MW, respectively.

Some structural characteristics of the French transmission network have been provided, including the following: mean node degree $\langle k \rangle$, maximum node degree $k_{\max}$, the mean shortest path $\langle l \rangle$, the cluster coefficient C, and the graph diameter d (Alipour et al. 2014). These characteristics suggest that the transmission network is a sparse network with average degree of 3.05, with a number of links $L = 220 \ll N^2 = 29{,}241$. The clustering coefficient of 0.279 and mean shortest path of 6.61 are both greater than what would be expected from a random network (Rosato et al. 2007), suggesting that the French transmission network is a small world network, where most nodes are not connected to one another but can be reached through a few nodes that play the role of "hubs." According to Rosato et al. (2007) and Solé et al. (2008), such a transmission

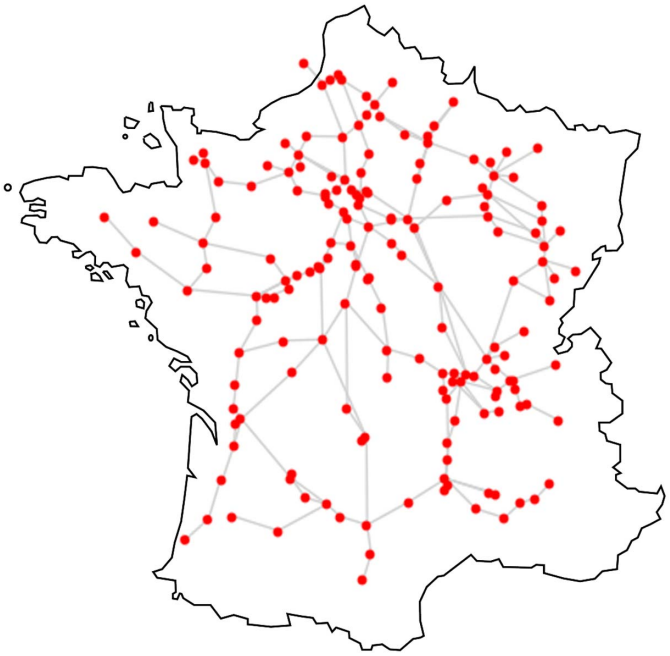

Fig. 2. 400-kV French power transmission network.

network is fragile to disruptive events. Consequently, identifying the most critical components and enhancing their adaptive capacity is of great significance to manage network resilience.

Simulated Disruption

To maximize the adaptive capacity of the 400-kV French transmission network, we extend an operational scenario to include information about (1) disrupted network components; (2) the level of disruptions; (3) number of available adaptive capacity resources; and (4) their impact on reducing the severity of disruptions. The spatial clusters to develop set S could be derived by a number of means, including government zones or decision making areas of authority. We make use of a clustering method, of which three were considered: hierarchical clustering, k-means clustering, and density based spatial clustering of application with noise (DBSCAN). In this application, there is an advantage of using DBSCAN over using other methods for potential locations allocation. The disrupted locations of the French 400-kV transmission network are scattered throughout the country. According to decision maker preferences and the horizon of the response phase, DBSCAN clusters the disrupted links that are accessible by a resource in the response phase time horizon. We assume that the total number of resources are sufficient for each possible set of clusters identified by DBSCAN, yet the number of each type of resource may not be sufficient for their assignment to all clusters. Unlike k-means and hierarchical clustering, DBSCAN relies on a density based notion and can identify clusters of arbitrary shape (Ester et al. 1996).

Start and end points are considered to be the objects that are geographically clustered. However, the lengths of the links in between are not equal, especially in transportation networks, and this inequality may lead to biased clustering. To avoid this issue, a set of virtual nodes generated links with equal unique length, an example of which is shown in Fig. 3 (Kriegel and Pfeifle 2005).

For illustrative purposes, a hypothetical spatially-confined scenario is assumed to occur within the northeast of France (e.g., an earthquake), as illustrated in Fig. 4. The disruptive event is assumed to be static (i.e., a design-based accident). DBSCAN classified the network into eight clusters, and outlier nodes are considered in their neighboring clusters. As the number of services each resource can send to disrupted links is limited, there are limitations in the number of disrupted links that each type of resource can fortify in each cluster. Hence, prioritizing components based on their criticality is of interest. It is assumed that 48% of links in the network are disrupted. There are four types of resources, $\{1, 2, 3, 4\}$, with (1) different fortifying process times, p^r, such that $(p^4 = 3) > (p^1 = 2) > (p^2 = 1) = (p^3 = 1)$, where each time period is half an hour; and (2) different fortifying capabilities are drawn from uniform distributions such that $H_{ij}^1 \in U(0.6, 0.75)$, $H_{ij}^2 \in U(0.45, 0.59)$, $H_{ij}^3 \in U(0.3, 0.44)$, $H_{ij}^4 \in U(0.15, 0.29)$. Examples of specifying resources and capabilities include (1) limiting the number of transformers that can be substituted with disrupted transformers temporarily (such transformers may not perform as well as the originals, yet can be substituted immediately after disruptions); (2) enhancing the black-start capacity of generators, which leads to partial performance of disrupted generators before they are returned to fully operational status in the network; and (3) adjusting or removing certain protective systems that may result in not using the whole residual network capacity in the aftermath of disruptions (e.g., undervoltage, underfrequency, synchronization checks) (National Research Council 2012).

The average number of available resources is $\bar{M}^r = 2$, and the average number of services is $\bar{U}^r = 3$. Table 1 illustrates the characteristics of each resource by indicating their effect on network performance if only one type of resource is used. Based on Table 1, the resource type $r = 3$ has the shortest processing time and the resource type $r = 1$ has the largest fortifying capability (i.e., the aggregate flow after the its implementation at $t = 3$, is larger than the aggregate flow resulting from the application of the other resources). Although resource type $r = 4$ has the longest processing time and the weakest fortification capability, this type of resource may be used in the absence of other types of resources.

Because of the nature of the short term response, the length of the adaptive capacity time horizon is much shorter than the recovery time horizon. Hence, we consider some assumptions to specify adaptive capacity characteristics: (1) when a resource, $r \in \{1, \ldots, R\}$, is assigned to a cluster, $s \in \{1, \ldots, S\}$, it cannot be reassigned to another cluster, $s' \in \{1, \ldots, S\}$; (2) discussed previously, the distance between any two clusters s', $s \in \{1, \ldots, S\}$ makes it impractical for a resource in one cluster to service the

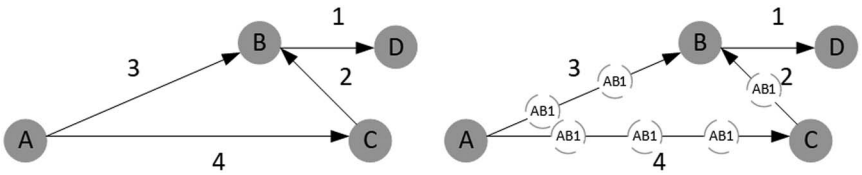

Fig. 3. Link division in a sample network.

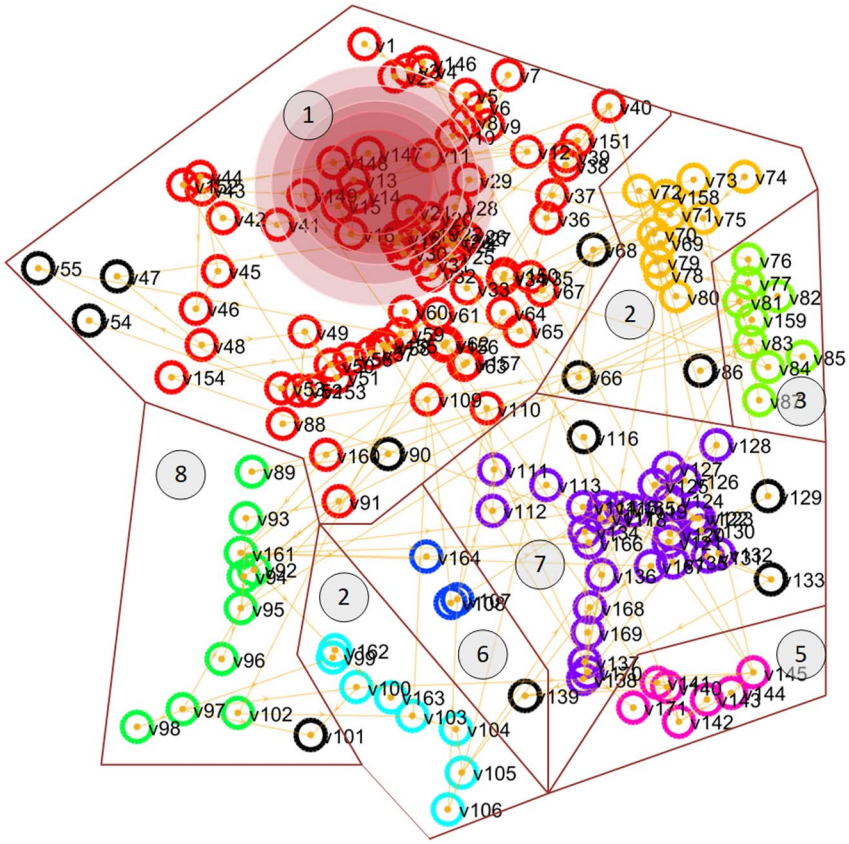

Fig. 4. French power transmission network divided into eight spatial clusters identified with DBSCAN, with spatial disruption centered in cluster $s = 1$.

Table 1. Aggregate flow across resources processing time $\boldsymbol{r} \in \{\mathbf{1}, \ldots, \boldsymbol{R}\}$

	Resource			
Processing time p^r	$r = 1$ 2	$r = 2$ 1	$r = 3$ 1	$r = 4$ 3
$t = 1$	2,158	2,158	2,158	2,158
$t = 2$	2,158	15,524	14,917	2,158
$t = 3$	16,700	26,965	25,805	2,158
$t = 4$	16,700	35,003	33,915	13,318
$t = 5$	29,751	42,473	38,863	13,318
$t = 6$	29,751	45,364	40,851	13,318
$t = 7$	40,467	45,837	40,912	21,249
$t = 8$	40,467	45,866	40,912	21,249

disrupted components in other clusters; (3) all services are released to serve disrupted components immediately after a disruptive event; and (4) when each service is assigned to a disrupted component, it cannot be reassigned to any other disrupted component.

Computational Experiment

The model provides the optimal solution for the 400-kV French transmission network and is solved with Python 2.7 using Gurobi 6.5.2. The computational time is in the order of few seconds, suggesting that the model is potentially useful for real-time post-disruption planning.

The subsequent analysis considers different importance measures for link criticality and different weights for demand nodes.

Link Criticality

As link importance measures, I_{ij}^{π}, were discussed generally in the section entitled "Criticality," earlier in this chapter, this application makes use of three (predisruption) flow-based importance measures that account for different perspectives on component contribution to network performance measure *all node pairs maximum flow* (Nicholson et al. 2016): (1) *max flow edge count* (I_{ij}^{MFcount}), or the total number of times a given edge is utilized in all *o-d* pairs max flow problems, (2) *edge flow centrality* (I_{ij}^{Flow}), or the sum of flow on $(i, j) \in A'$ for all possible *o-d* pair max flow problems divided by the sum of all pairs max flows [a variation on the node centrality measure by Freeman et al. (1991)], and (3) *flow capacity rate* (I_{ij}^{FCR}), or a measure of how close $(i, j) \in A'$ is to becoming a potential bottleneck based on the difference between max flow amount and capacity. We also consider a scenario where no importance measure is assumed, our concern is only the second element of objective function. Analyses described subsequently will illustrate how these different perspectives alter adaptive capacity strategies.

Weights for Demand Nodes and Time Periods

We define two corresponding time-based weight procedures. *Descending scaled weight* is defined by placing more importance on adding adaptive capacity in earlier time periods (e.g., $\mu_h > \mu_l$, for $\forall h < l$ when $h, l \in \{1, \ldots, T\}$, $\mu_h = 1 - [h/(T + 1)]$). *Ascending scaled weight* is defined by placing more attention on network performance in later time periods (e.g., $\mu_h > \mu_l$, for $\forall h > l$, when $h, l \in \{1, \ldots, T\}$, $\mu_h = 1 + [h/(T + 1)]$), such that the transition to restoration may occur more smoothly.

J. Infrastruct. Syst., 2018, 24(4): 04018022

Table 2. Aggregate flow, number of active links, and demand nodes receiving flow across link importance measures: μ_t and w_i constant

Time	I^{MFcount}	I^{Flow}	I^{FCR}	Constant
$t = 1$	2,158	2,158	2,158	2,158
$t = 2$	6,968	6,968	7,100	6,968
$t = 3$	20,305	20,362	20,233	20,305
$t = 4$	26,843	26,815	26,902	26,843
$t = 5$	35,090	35,222	34,814	35,090
$t = 6$	37,366	37,377	37,169	37,366
$t = 7$	42,877	42,706	42,745	42,877
$t = 8$	43,105	42,952	42,973	43,105
D_{iT} (total active demand node)	140	139	139	138
E_{ijT} (total active links)	201	199	196	203
Fortified critical components	29	27	27	26

Table 3. Aggregate flow, number of active links, and demand nodes receiving flow across link importance measures: μ_t constant and w_i scaled

Time	I^{MFcount}	I^{Flow}	I^{FCR}	Constant
$t = 1$	2,158	2,158	2,158	2,158
$t = 2$	5,190	4,872	4,884	5,190
$t = 3$	17,339	16,965	17,489	17,339
$t = 4$	23,985	23,604	23,903	23,588
$t = 5$	33,074	33,524	33,135	33,903
$t = 6$	35,954	35,754	35,696	36,617
$t = 7$	41,992	41,983	41,738	41,738
$t = 8$	42,220	42,098	41,966	41,966
D_{iT} (total active demand node)	134	136	137	136
E_{ijT} (total active links)	189	200	202	205
Fortified critical components	26	24	25	22

As for the weights of the demand nodes, w_i, $i \in N_-$, we consider scaled weights (i.e., specific to particular demand nodes), and constant weights (i.e., that assume similar importance across demand nodes). As such, we explore how focusing on meeting demand in particularly critical demand nodes alters adaptive capacity strategies. The scaled weights of demand nodes are utilized such that nodes in high populated areas are of greater significance than others (e.g., demand nodes are divided into two categories, relatively high populated demand nodes, and relatively low populated areas). The weight of demand nodes in high populated areas are as twice that of demand nodes located in low populated areas.

Computational Results

Tables 2–7 present results of the adaptive capacity formulation on the French power network example, including (1) the aggregate flow in each time period, calculated as $\sum_{i \in N_-} \varphi_{it}$; (2) the number of links that are active at time period T, calculated as $\sum_{(i,j) \in A'} E_{ijT}$, where E_{ijT} is a binary variable that is 1 if $x_{ijT} > 0$ and 0 otherwise; and (3) the number of demand nodes that receive flow, calculated as $\sum_{i \in N_-} D_{iT}$, where D_{iT} is a binary variable that is 1 if $\varphi_{iT} > 0$ and 0 otherwise.

The effects of the three weights are examined: w_i, $i \in N_-$ for weighting the importance of demand nodes, μ_t, $t \in \{1, \ldots, T\}$ for weighting network performance in each time period, and I_{ij}^{π} for expressing the criticality of links. Each take on either a scaled value (following a specific calculation) or a constant value (all times periods, links, or demand nodes are weighted equally).

Constant weights, $w_i = 1$ and $\mu_t = 1$, for the demand node and time periods in Table 2 model the objective to pass maximum power throughout the residual network. Therefore, the model delivers maximum flow at the end of the fortification phase, in comparison to the maximum flow delivered at the end of fortification phase in Tables 2–6. As shown in Table 2, there is a potential issue in applying importance measures in the model formulation when constant weights are used (i.e., similar results are achieved by not using any importance measure and by using I_{ij}^{MFcount}). On the other hand, the use of the other importance measures resulted in decreased performance of the adaptive capacity strategies. That is because the goal of fortification is to adapt to the immediate adverse impact of the disruption. Therefore, each fortified link is not going to be fully functional until the end of the longer-term recovery process, which reduces the efficiency of using the importance measures in the model in the short term. However, fortifying links with a higher criticality may not improve the

Table 4. Aggregate flow, number of active links, and demand nodes receiving flow across link importance measures: μ_t ascending and w_i constant

Time	I^{MFcount}	I^{Flow}	I^{FCR}	Constant
$t = 1$	2,158	2,158	2,158	2,158
$t = 2$	6,968	6,687	6,968	6,968
$t = 3$	20,305	20,411	20,388	20,362
$t = 4$	26,843	26,856	26,872	26,815
$t = 5$	35,109	35,263	35,234	34,927
$t = 6$	37,368	37,455	37,476	37,295
$t = 7$	42,877	42,540	42,480	42,877
$t = 8$	43,105	42,768	42,776	43,105
D_{iT} (total active demand node)	140	139	140	139
E_{ijT} (total active links)	194	207	194	200
Fortified critical components	28	23	23	23

Table 5. Aggregate flow, number of active links, and demand nodes receiving flow across link importance measures: μ_t descending and w_i constant

Time	I^{MFcount}	I^{Flow}	I^{FCR}	Constant
$t = 1$	2,158	2,158	2,158	2,158
$t = 2$	7,291	6,968	6,968	7,100
$t = 3$	20,332	20,388	20,277	20,351
$t = 4$	27,116	27,007	26,856	26,778
$t = 5$	34,937	35,328	35,185	35,263
$t = 6$	36,705	37,112	37,456	37,456
$t = 7$	42,589	42,502	42,493	42,646
$t = 8$	42,837	42,602	42,572	42,739
D_{iT} (total active demand node)	137	145	138	137
E_{ijT} (total active links)	192	196	196	197
Fortified critical components	27	24	25	24

Table 6. Aggregate flow, number of active links, and demand nodes receiving flow across link importance measures: μ_t ascending and w_i scaled

Time	I^{MFcount}	I^{Flow}	I^{FCR}	Constant
$t = 1$	2,158	2,158	2,158	2,158
$t = 2$	4,884	4,884	4,884	4,884
$t = 3$	17,033	17,489	17,033	17,033
$t = 4$	23,985	23,024	23,302	23,985
$t = 5$	33,250	34,018	32,494	34,018
$t = 6$	35,954	36,875	35,549	36,875
$t = 7$	41,992	41,992	41,738	41,992
$t = 8$	42,220	42,220	41,966	42,220
D_{iT} (total active demand node)	136	134	136	134
E_{ijT} (total active links)	199	194	196	212
Fortified critical components	28	26	26	26

Table 7. Aggregate flow, number of active links, and demand nodes receiving flow across link importance measures: μ_t descending and w_i scaled

Time	I^{MFcount}	I^{Flow}	I^{FCR}	Constant
$t = 1$	2,158	2,158	2,158	2,158
$t = 2$	6,700	6,700	6,700	6,700
$t = 3$	18,038	18,037	18,038	18,038
$t = 4$	24,602	23,746	24,471	24,601
$t = 5$	32,949	32,949	32,949	32,949
$t = 6$	34,572	34,572	34,456	34,571
$t = 7$	39,717	39,752	39,260	39,596
$t = 8$	39,736	39,770	39,260	39,615
D_{iT} (total active demand node)	133	130	130	131
E_{ijT} (total active links)	190	194	193	195
Fortified critical components	26	24	24	24

network performance during the short term assessed in this study (i.e., $t \le t_d$), but as the critical links priorities in response phase are higher than other links (i.e., the coefficient of critical links in the objective function are greater than other links) they are going to be proportionally recovered at the beginning of recovery phase (i.e., $t > t_d$), which may enhance the recovery process.

Among the implemented importance measures, I_{ij}^{MFcount} shows the best performance in guiding the fortification of links as it identifies components that are shared in the maximum number of source-sink paths regardless of the percentage of the network flow that the component carries in the network. Hence, fortifying the components with maximum I_{ij}^{MFcount} brings a great number of disrupted paths into partial activation. However, as the outcome of the response phase is to proportionally restore components, the links that are important according to I_{ij}^{Flow} and I_{ij}^{FCR} in the fully operational network may not be identified as critical in the fortified network. This is due to the fact that their capacity is not necessarily fully exploited in the partially operational network.

Fortifying links with a higher criticality may not improve the network performance during the short term assessed in this study (i.e., $t \le t_d$), but as the critical link priorities in response phase are higher than other links (i.e., the first part of the objective function), they are going to be proportionally recovered at the beginning of recovery phase (i.e., $t > t_d$). This may enhance the recovery process. For example, Tables 2–7 suggest that the implementation of importance measures may not always result in better network performance. However, when compared to the conditions where only the second element of the objective function is considered, the application of the importance measures increases the number fortified critical components and reduces the long-term recovery horizon resulting in increased system resilience.

From the comparison of Table 2 with Tables 3, 6, and 7, it appears that the priority weights of demand nodes have negative effects on the short-term response. Nurre et al. (2012) mention that a "priority-based" plan, where w_i is scaled, is aligned with a "demand-based" long-term recovery plan, where restoration efforts minimize the total demand dissatisfaction in the network (i.e., "priority-based" is also an optimal solution for the model with the "demand-based" restoration formulation). However, when we consider scaled w_i in strengthening the short-term adaptive capacity, the same results are not observed because the length of the time horizon, $t_e < t < t_d$, is not extended enough to fulfill the resource allocation to all the prioritized demand nodes. Due to the interplay between the incomplete short-term response and the assumed characteristics of the resources, the priority-based results of this study conflict with the general priority-based results from the literature. However, in Table 3, applying importance measures to the model with scaled demand node weights leads to results that are more aligned with the demand-based formulation, where the goal is to maximize the aggregate flow reaching to demand nodes. In Table 3, the application of importance measures enhances adaptive capacity, suggesting that the aggregate flow increases (i.e., the total unsatisfied demand decreases), and the total D_{iT} increases (the number of demand nodes receiving flow increases). Recall that the importance measures lead the model to maximize the aggregate flow as well as the number of satisfied prioritized demand nodes by focusing on the links that are responsible for a large proportion of flow in the network.

In the limited time horizon, the goal of fortifying adaptive capacity is to reach the maximum possible performance of the demand nodes (aggregate flow) at any time step $t \in \{1, \ldots, T\}$. One might imagine that the level of network performance at time T is of a greater significance than prior time periods as longer term recovery follows. Therefore, the higher level of network performance at time T may lead to more effective recovery. However, in some case studies, reaching a certain level of aggregate flow earlier is more important than reaching the maximum fortified level of performance at time T (e.g., nodes that include hospitals are required to receive power as soon as possible). Based on Table 3, ascending μ_t puts more emphasis on aggregate flow at the end of the response horizon, while in Table 4, descending μ_t places emphasis on increasing aggregate flow in earlier time periods. Note that it is assumed that there exists a tradeoff for resource capability and processing time: resources have shorter processing time with less fortification capabilities (e.g., $r = 3$ in Table 1), or they have stronger fortification capabilities with more processing time (e.g., $r = 1$ in Table 1). From Tables 4 and 5, we conclude that reaching to a certain level of performance (ascending and descending μ_t) in a short period of time might not be aligned with the implementation of importance measures. Indeed, in the response phase, the fortified portion of the capacity of less important links may carry a greater amount of flow than the partially operational critical links.

In Table 5, using importance measures may distribute the same amount of aggregate flow among more demand nodes. This may result in fewer demand nodes being satisfied. However, depending on the temporal importance of fortification, a higher level of demand could be met for vital activities (e.g., hospitals, evacuation of casualties in particular areas). The similarity of Tables 4 and 6 suggests that the same level of demand over the response horizon is met using either a constant μ_t or an ascending μ_t in conjunction with a scaled w_i. A comparison of Tables 5 and 7 suggests that implementing a scaled value of w_i performs better when no scale is given to time periods with μ_t, though the comparison of Tables 5 and 7 suggests that if a descending μ_t is used, then demand is met more effectively with a constant w_i. We note from Tables 2–7 that E_{ijT}, the number of links used to achieve aggregate flow, decreases when importance measures are applied. This might be of importance in situations when it is preferred to use fewer links and consequently shorter paths. For instance, in Table 6 using I_{ij}^{MFcount} in the model delivers the more aggregate flow with fewer links relative to using no importance measure.

Resource Allocation Sensitivity Analysis

As adaptive-capacity-enhancing resources are limited, two scenarios are developed to alter $\bar{M}^r$, the average number of resources available, and $\bar{U}^r$, the average number of services that can be released from resources and assigned to disrupted components. The two scenarios applied to the French power network are: (1) a varying number of services that each resource can send to disrupted

J. Infrastruct. Syst., 2018, 24(4): 04018022

Table 8. The impact of the average number of resources $\bar{M}^r$ on aggregate flow, number of active links, and demand nodes receiving flow: constant μ_t, constant w_i

	$\bar{M}^r$							
Time	1	2	3	4	5	6	7	8
$t = 1$	0	0	0	0	0	0	0	0
$t = 2$	3,491	5,811	10,157	14,288	14,336	14,061	14,336	13,511
$t = 3$	7,846	15,557	21,929	23,635	23,699	24,051	23,660	24,442
$t = 4$	11,684	24,513	29,125	32,803	32,998	33,060	32,906	33,641
$t = 5$	14,562	31,251	38,194	40,390	40,463	40,196	40,828	40,543
$t = 6$	14,562	33,639	42,079	43,108	42,927	43,908	44,206	44,627
$t = 7$	16,903	39,363	45,815	44,776	43,923	44,776	45,347	45,698
$t = 8$	16,903	39,479	45,931	44,776	45,931	45,931	45,347	45,698
Total D_{iT}	128	137	137	139	139	139	139	140
Total E_{ijT}	198	215	210	204	197	202	200	205

links from the range $\bar{U}^r \in (0, \lceil |A|/S \rceil)$; and (2) a specific number of available resources of each type $\bar{M}^r \in (0, S)$.

Table 8 indicates the impact of number of resources on aggregate flow and the number of demand nodes which receive flow, respectively. Results indicate that when $\bar{M}^r \geq 5$, the MILP obtains the best solution, higher aggregate flow, as well as more satisfied demand nodes, and increasing the average number of resources to more than four will not impact on the total amount aggregate flow reaching to the demand nodes. We do note that the required number of resource depends on the topology of the network, number of important links which are affected, and the location of the disruptive event (e.g., the epicenter of the earthquake).

Table 9 indicates the impact of resource capacity on the aggregate flow, number of demand nodes receiving flow, and number of involved links, respectively, for ascending μ_t and constant w_i. The results are analyzed under ascending μ_t and scaled w_i and suggest that increasing capacity of resources enables the model to maximize aggregate flow and serves more demand nodes. However, for each of eight time periods in Table 9, there is a threshold in average number of services each resource can release to disrupted components ($\bar{U}^r = 10$) above which no more improvement is seen in the aggregate flow reaching to the demand nodes. Table 10 shows the impact of resource capacity on the aggregate flow, number of demand nodes receiving flow, and number of involved links, respectively, for constant μ_t and scaled w_i. When demand nodes are prioritized (w_i is scaled), $\bar{U}^r = 9$ is the optimal solution for the model as it represents the maximum aggregate flow reaching to demand nodes, which is less than the situation in which there is no priority weights for demand nodes.

Concluding Remarks

This work is an initial attempt to explore the assignment of resources to a disrupted infrastructure network to enhance its adaptive capacity, or the ability of the network to quickly adapt after a disruption by temporary means. The MILP formulation proposed here uniquely accounts for three characteristics: (1) link criticality, to emphasize those links that are considered important to the network; (2) vulnerability, to emphasize those links that enable flow in the network; and (3) connectivity, to emphasize those links that enable demand to be met at demand nodes. The optimization formulation

Table 9. The impact of the average number of services released from resources $\bar{U}^r$ on aggregate flow, number of active links, and demand nodes receiving flow: ascending μ_t, constant w_i

	$\bar{U}^r$										
Time	3	4	5	6	7	8	9	10	11	12	13
$t = 1$	2,158	2,158	2,158	2,158	2,158	2,158	2,158	2,158	2,158	2,158	2,158
$t = 2$	6,968	8,617	9,872	11,090	12,426	13,379	13,865	14,444	14,928	14,928	14,928
$t = 3$	20,305	24,961	29,692	32,709	34,559	36,032	38,118	38,649	39,692	39,861	40,184
$t = 4$	26,843	31,732	35,724	38,976	40,617	42,577	42,943	44,430	46,163	46,442	46,765
$t = 5$	35,090	40,795	43,131	44,677	46,144	46,518	46,645	46,871	47,066	47,120	47,120
$t = 6$	37,366	41,273	43,131	44,677	46,144	46,518	46,645	46,871	47,066	47,120	47,120
$t = 7$	42,877	45,496	46,631	46,947	46,918	47,065	47,120	47,120	47,120	47,120	47,120
$t = 8$	43,107	45,496	46,631	46,947	46,918	47,065	47,120	47,120	47,120	47,120	47,120
Total D_{iT}	139	140	140	142	141	143	204	143	143	143	143
Total E_{ijT}	197	203	209	201	206	209	143	207	205	210	208

Table 10. The impact of the average number of services released from resources $\bar{U}^r$ on the aggregate flow, number of active links, and demand nodes receiving flow: constant μ_t, scaled w_i

	$\bar{U}^r$										
Time	3	4	5	6	7	8	9	10	11	12	13
$t = 1$	2,158	2,158	2,158	2,158	2,158	2,158	2,158	2,158	2,158	2,158	2,158
$t = 2$	5,190	6,549	8,833	12,034	12,034	13,170	13,170	18,325	18,528	5,190	6,549
$t = 3$	17,339	21,801	26,270	33,023	33,023	34,516	34,516	36,900	37,605	21,339	21,801
$t = 4$	23,588	31,171	34,301	38,516	38,516	39,778	39,778	42,048	42,818	33,588	31,171
$t = 5$	33,903	39,077	42,283	44,028	44,028	44,508	44,508	45,355	45,353	45,355	45,353
$t = 6$	36,616	39,772	42,287	44,028	44,028	44,508	44,508	45,355	45,353	45,355	45,353
$t = 7$	41,738	44,231	44,485	45,177	45,177	45,177	45,177	45,473	45,473	45,473	45,473
$t = 8$	41,966	44,231	44,485	45,177	45,177	45,177	45,177	45,473	45,473	45,473	45,473
Total D_{iT}	135	139	140	142	141	143	143	143	143	143	143
Total E_{ijT}	201	212	209	197	197	209	206	205	211	210	208

J. Infrastruct. Syst., 2018, 24(4): 04018022

was applied to a spatial disruption of the topology of the 400 kV French network.

To measure link criticality, three flow-driven importance measures from Nicholson et al. (2016) were used and their effect on the aggregate flow, number of demand nodes receiving flow, and number of involved links were measured. These measures emphasize the effects of the links in the network to the maximum flow in each time period from different perspectives, though any type of network importance measure could be used. Note these importance measures may provide a limited perspective, as adaptive capacity is assumed to not fully recover disruptions. However, from an integrated approach, fortifying more important links in the short term may result in more effective recovery in terms of length of recovery time and the quality of recovery plan. All resources are assigned to clusters immediately after the disruption. However, further work is needed to explore how quickly after a disruption adaptive capacity resources can be engaged to determine the value of postdisruption importance information.

We examine the adaptive capacity efforts of the network when there are priorities of decision makers of the power network. It is observed that the optimal solution cannot be aligned with demand node priority as the network cannot be completely recovered during the short term and the component which is fortified by resources to lead flow through more important demand nodes may differ from the component which provide maximum aggregate flow in each time period. Ascending time weight, μ_t, aligns with maximum aggregate flow optimal solution. Furthermore, it provides the optimal solution that maximizes network performance at the end of the adaptive capacity time horizon, T, which may consequently lead to more effective recovery. Regarding component criticality, the computational results suggest that the implementation of I_{MFcount} under any strategy (i.e., constant or scaled μ_t and w_i) enhance the adaptive capacity. In situations when demand nodes are prioritized, the use of the importance measures assists in choosing the paths that satisfy the corresponding demand nodes while considering the performance of the whole network.

A direction for future work is the integration of the vulnerability reduction formulation proposed here with a restoration formulation, effectively studying the tradeoff between resource assignment for adaptive capacity versus restorative capacity for more comprehensive network resilience planning under dynamic disruption scenarios.

Notation

The following symbols are used in this paper:

A = set of links in network $G = (N, A)$;
$A' \subseteq A$ = set of disrupted links in network $G = (N, A)$;
b_i = amount of demand in each node $i \in N_-$ in each time period;
I_{ij}^{π} = importance measure calculated for $(i, j) \in A$ of type π;
N = set of nodes in network $G = (N, A)$;
$N_- \subseteq N$ = set of demand nodes in network $G = (N, A)$;
$N_+ \subseteq N$ = set of supply nodes in network $G = (N, A)$;
$N_= \subseteq N$ = set of transition nodes in network $G = (N, A)$;
M^r = number of available resources of type $r = 1, \ldots, R$;
o_i = amount of supply in each node $i \in N_+$ in each time period;
p^r = fortification time of each service sent from resource $r = 1, \ldots, R$ to each disrupted link;
$r = 1, \ldots, R$ = set of resources;
$s = 1, \ldots, S$ = set of clusters;
U^r = number of services each resource $r = 1, \ldots, R$ can send to disrupted components after its allocation to a particular cluster;
u_{ijt_e} = capacity of each link $(i, j) \in A$ before the disruption;
u_{ijt_d} = capacity of each link $(i, j) \in A'$ after the disruption (assuming no fortification);
V_{ijt} = measure of accessibility (fortified capacity) associated with disrupted link (i, j);
w_i = importance weight assigned to demand node i;
x_{ijt} = continuous variable representing the flow on link $(i, j) \in A$ at time t;
y_{ijt}^{rs} = binary variable equal to 1 if a service of resource r assigned to cluster s finishes the fortification process of link $(i, j) \in A'$ at time $t = 1, \ldots, T$;
z^{rs} = binary variable equal to 1 if resource r is assigned to cluster s;
θ_{ij}^{s} = binary parameter equal to 1 if link $(i, j) \in A'$ belongs to cluster $s = 1, \ldots, S$ and 0 otherwise;
μ_t = weight associated with the performance of the network in each time t;
φ_{it} = continuous variable representing the amount of flow reaching to demand node $i \in N_-$ at each time t; and
φ_{it_e} = aggregate flows reaching node $i \in N_-$ before the disruption.

References

Akbari, V., and F. S. Salman. 2017. "Multi-vehicle synchronized arc routing problem to restore post-disaster network connectivity." *Eur. J. Oper. Res.* 257 (2): 625–640. https://doi.org/10.1016/j.ejor.2016.07.043.

Aksu, D. T., and L. Ozdamar. 2014. "A mathematical model for post-disaster road restoration: Enabling accessibility and evacuation." *Transp. Res. Part E Logist. Transp. Rev.* 61: 56–67. https://doi.org/10.1016/j.tre.2013.10.009.

Albert R., I. Albert, and G. L. Nakarado. 2004. "Structural vulnerability of the North American power grid." *Phys. Rev. E.* 69 (2): 025103. https://doi.org/10.1103/PhysRevE.69.025103.

Aldrich, D. P. 2012. *Building resilience: Social capital in post-disaster recovery.* Chicago: University of Chicago Press.

Alipour, Z., M. A. S. Monfared, and E. Zio. 2014. "Comparing topological and reliability-based vulnerability analysis of Iran power transmission network." *J. Risk Reliab.* 228 (2): 139–151. https://doi.org/10.1177/1748006X13501652.

Arab, A., A. Khodaei, S. K. Khator, and Z. Han. 2015. "Transmission network restoration considering AC power flow constraints." In *Proc., 2015 IEEE Int. Conf. on Smart Grid Communications*. 816–821. Piscataway, NJ: IEEE.

Arab, A., A. Khodaei, S. K. Khator, and Z. Han. 2016. "Electric power grid restoration considering disaster economics." *IEEE Access* 4: 639–649. https://doi.org/10.1109/ACCESS.2016.2523545.

Arghandeh, R., A. V. Meier, L. Mehrmanesh, and L. Mili. 2016. "On the definition of cyber-physical resilience in power systems." *Renewable Sustainable Energy Rev.* 58: 1060–1069. https://doi.org/10.1016/j.rser.2015.12.193.

ASCE. 2017. "Report card for America's infrastructure." Accessed December 10, 2017. https://www.infrastructurereportcard.org/.

Aven, T. 2011. "On some recent definitions and analysis frameworks for risk, vulnerability, and resilience." *Risk Anal.* 31 (4): 515–522. https://doi.org/10.1111/j.1539-6924.2010.01528.

Averbakh, I. 2012. "Emergency path restoration problems." *Discrete Optim.* 9 (1): 58–64. https://doi.org/10.1016/j.disopt.2012.01.001.

Averbakh, I., and J. Pereira. 2012. "The flowtime network construction problem." *IIE Trans.* 44 (8): 681–694. https://doi.org/10.1080/0740817X.2011.636792.

Barker, K., J. E. Ramirez-Marquez, and C. M. Rocco. 2013. "Resilience-based network component importance measures." *Reliab. Eng. Syst. Saf.* 117: 89–97. https://doi.org/10.1016/j.ress.2013.03.012.

Berdica, K., and L. G. Mattsson. 2007. "Vulnerability: A model-based case study of the road network in Stockholm." In *Critical infrastructure: Reliability and vulnerability*, edited by A. T. Murray and T. H. Grubesic, 81–106. New York: Springer.

Bye, P. 2013. Vol. 753 of *A pre-event recovery planning guide for transportation*. Washington, DC: Transportation Research Board.

Çelik, M., Ö. Ergun, and P. Keskinocak. 2015. "The post-disaster debris clearance problem under incomplete information." *Oper. Res.* 63 (1): 65–85. https://doi.org/10.1287/opre.2014.1342.

Chen, X. Z., Q. C. Lu, Z. R. Peng, and J. E. Ash. 2015. "Analysis of transportation network vulnerability under flooding disasters." *Transp. Res. Rec.: J. Transp. Res. Board* 2532: 37–44.

Cimellaro, G., A. Reinhorn, and M. Bruneau. 2010. "Seismic resilience of a hospital system." *Struct. Infrastruct. Eng.* 6 (1): 127–144. https://doi.org/10.1080/15732470802663847.

Cohen, R., K. Erez, D. Ben-Avraham, and S. Havlin. 2000. "Resilience of the internet to random breakdowns." *Phys. Rev. Lett.* 85 (21): 4626–4628. https://doi.org/10.1103/PhysRevLett.85.4626.

Cooper, J. D., I. M. Fiedland, I. G. Buckle, R. B. Nimis, and N. McMullin Bobb. 1994. "The Northridge earthquake: Progress made, lessons learned in seismic-resistant bridge design." *Public Roads* 58 (1): 26–36.

Cutter, S. L., K. D. Ash, and C. T. Emrich. 2014. "The geographies of community disaster resilience." *Global Environ. Change* 29: 65–77. https://doi.org/10.1016/j.gloenvcha.2014.08.005.

Demirel, H., M. Kompil, and F. Nemry. 2015. "A framework to analyze the vulnerability of European road networks due to sea-level rise (SLR) and sea storm surges." *Transp. Res. Part A: Policy Pract.* 81: 62–76. https://doi.org/10.1016/j.tra.2015.05.002.

DHS (Department of Homeland Security). 2013. *National infrastructure protection plan*. Washington, DC: Office of the Secretary of Homeland Security.

Division of Emergency Management. 2008. "2008–2013 strategic plan." Accessed December 10, 2017. www.floridadisaster.org.

Duque, P. A. M., I. S. Dolinskaya, and K. Sörensen. 2016. "Network repair crew scheduling and routing for emergency relief distribution problem." *Eur. J. Oper. Res.* 248 (1): 272–285. https://doi.org/10.1016/j.ejor.2015.06.026.

El-Rashidy, R. A., and S. M. Grant-Muller. 2014. "An assessment method for highway network vulnerability." *J. Transp. Geogr.* 34: 34–43. https://doi.org/10.1016/j.jtrangeo.2013.10.017.

Erath, A., M. Löchl, and K. W. Axhausen. 2009. "Graph-theoretical analysis of the Swiss road and railway networks over time." *Networks Spatial Econ.* 9 (3): 379–400. https://doi.org/10.1007/s11067-008-9074-7.

Ester, M., H. P. Kriegel, J. Sander, and X. Xu. 1996. "A density-based algorithm for discovering clusters in large spatial databases with noise." In *Proc., 2nd Int. Conf. Knowledge Discovery and Data Mining*, 226–231. Palo Alto, CA: Association for the Advancement of Artificial Intelligence.

Fang, Y. P., N. Pedroni, and E. Zio. 2014. "Comparing network-centric and power flow models for the optimal allocation of link capacities in a cascade-resilient power transmission network." *IEEE Syst. J.* 99: 1–12.

Fang, Y. P., and G. Sansavini. 2017. "Optimizing power system investments and resilience against attacks." *Reliab. Eng. Syst. Saf.* 159: 161–173. https://doi.org/10.1016/j.ress.2016.10.028.

Francis, R., and B. Bekera. 2014. "A metric and frameworks for resilience analysis of engineered and infrastructure systems." *Reliab. Eng. Syst. Saf.* 121 (1): 90–103. https://doi.org/10.1016/j.ress.2013.07.004.

Freeman, L. C., S. P. Borgatti, and D. R. White. 1991. "Centrality in valued graphs: A measure of betweenness based on network flow." *Social Networks* 13 (2): 141–154.

Ghasemi, M. A., and M. Parniani. 2016. "Prevention of distribution network overvoltage by adaptive droop-based active and reactive power control of PV systems." *Electr. Power Syst. Res.* 133: 313–327. https://doi.org/10.1016/j.epsr.2015.12.030.

Görmez, N., M. Köksalan, and F. S. Salman. 2011. "Locating disaster response facilities in Istanbul." *J. Oper. Res. Soc.* 62 (7): 1239–1252.

Haimes, Y. Y. 2009. "On the definition of resilience in systems." *Risk Anal.* 29 (4): 498–501. https://doi.org/10.1111/j.1539-6924.2009.01216.

Hansen, W. G. 1959. "How accessibility shapes land use." *J. Am. Inst. Planners* 25 (2): 73–76. https://doi.org/10.1080/01944365908978307.

Henry, D., and J. E. Ramirez-Marquez. 2012. "Generic metrics and quantitative approaches for system resilience as a function of time." *Reliab. Eng. Syst. Saf.* 99: 114–122. https://doi.org/10.1016/j.ress.2011.09.002.

Holme, P., B. J. Kim, C. N. Yoon, and S. K. Han. 2002. "Attack vulnerability of complex networks." *Phys. Rev. E* 65 (5): 056109. https://doi.org/10.1103/PhysRevE.65.056109.

Holmgren, A. J. 2006. "Using graph models to analyze the vulnerability of electric power networks." *Risk Anal.* 26 (4): 955–969.

Hosseini, S., and K. Barker. 2016. "A Bayesian network model for resilience-based supplier selection." *Int. J. Prod. Econ.* 180: 68–87. https://doi.org/10.1016/j.ijpe.2016.07.007.

Hosseini, S., K. Barker, and J. E. Ramirez-Marquez. 2016. "A review of definitions and measures of system resilience." *Reliab. Eng. Syst. Saf.* 145: 47–61. https://doi.org/10.1016/j.ress.2015.08.006.

Jacobson, E. U., N. T. Argon, and S. Ziya. 2012. "Priority assignment in emergency response." *Oper. Res.* 60 (4): 813–832. https://doi.org/10.1287/opre.1120.1075.

Jenelius, E., and L. G. Mattsson. 2012. "Road network vulnerability analysis of area-covering disruptions: A grid-based approach with case study." *Transp. Res. Part A: Policy Pract.* 46 (5): 746–760.

Jenelius, E., and L. G. Mattsson. 2015. "Road network vulnerability analysis: Conceptualization, implementation and application." *Comput. Environ. Urban Syst.* 49: 136–147. https://doi.org/10.1016/j.compenvurbsys.2014.02.003.

Jenelius, E., T. Petersen, and L. G. Mattsson. 2006. "Importance and exposure in road network vulnerability analysis." *Transp. Res. Part A: Policy Pract.* 40 (7): 537–560. https://doi.org/10.1016/j.tra.2005.11.003.

Johansson, J., and H. Hassel. 2010. "An approach for modelling interdependent infrastructures in the context of vulnerability analysis." *Reliab. Eng. Syst. Saf.* 95 (12): 1335–1344.

Johansson, J., H. Hassel, and A. Cedergren. 2011. "Vulnerability analysis of interdependent critical infrastructures: Case study of the Swedish railway system." *Int. J. Crit. Infrastruct.* 7 (4): 289–316. https://doi.org/10.1504/IJCIS.2011.045065.

Jonsson, H., J. Johansson, and H. Johansson. 2008. "Identifying critical components in technical infrastructure networks." *J. Risk Reliab.* 222 (2): 235–243.

Kasaei, M., and F. S. Salman. 2016. "Arc routing problems to restore connectivity of a road network." *Transp. Res. Part E Logist. Transp. Rev.* 95: 177–206. https://doi.org/10.1016/j.tre.2016.09.012.

Kriegel, H. P., and M. Pfeifle. 2005. "Density-based clustering of uncertain data." In *Proc., 11th ACM SIGKDD Int. Conf. on Knowledge Discovery in Data Mining*, 672–677. New York: ACM.

Lempert, R. J., and D. G. Groves. 2010. "Identifying and evaluating robust adaptive policy responses to climate change for water management agencies in the American west." *Technol. Forecasting Social Change* 77 (6): 960–974. https://doi.org/10.1016/j.techfore.2010.04.007.

MacKenzie, C. A., K. Barker, and F. H. Grant. 2012. "Evaluating the consequences of an inland waterway port closure with a dynamic multiregional interdependency model." *IEEE Trans. Syst. Man Cybern. Part A Syst. Hum.* 42 (2): 359–370.

Magis, K. 2010. "Community resilience: An indicator of social sustainability." *Soc. Nat. Resour.* 23 (5): 401–416. https://doi.org/10.1080/08941920903305674.

Morris, J. M., P. L. Dumble, and M. R. Wigan. 1979. "Accessibility and indicators for transport planning." *Transp. Res. Part A* 13 (2): 91–109. https://doi.org/10.1016/0191-2607(79)90012-8.

Nagurney, A., and Q. Qiang. 2007a. "A network efficiency measure for congested networks." *Europhys. Lett.* 79: 38005.

Nagurney, A., and Q. Qiang. 2007b. "Robustness of transportation networks subject to degradable links." *Europhys. Lett* 80: 68001.

Nagurney, A., and Q. Qiang. 2008. "A network efficiency measure with application to critical infrastructure networks." *J. Global Optim.* 40 (1–3): 261–275.
Nan, C., and G. Sansavini. 2017. "A quantitative method for assessing resilience of interdependent infrastructures." *Reliab. Eng. Syst. Saf.* 157: 35–53. https://doi.org/10.1016/j.ress.2016.08.013.
Newman, M. E. 2005. "A measure of betweenness centrality based on random walks." *Social Networks* 27 (1): 39–54.
Nicholson, C. D., K. Barker, and J. E. Ramirez-Marquez. 2016. "Flow-based vulnerability measures for network component importance: Experimentation with preparedness planning." *Reliab. Eng. Syst. Saf.* 145: 62–73. https://doi.org/10.1016/j.ress.2015.08.014.
NRC (National Research Council). 2012. *Terrorism and the electric power delivery system*. Washington, DC: National Academies Press.
Nurre, S. G., B. Cavdaroglu, J. E. Mitchell, and T. C. Sharkey. 2012. "Restoring infrastructure systems: An integrated network design and scheduling (INDS) problem." *Eur. J. Oper. Res.* 223 (3): 794–806.
Nurre, S. G., and T. C. Sharkey. 2014. "Integrated network design and scheduling problems with parallel identical machines: Complexity results and dispatching rules." *Networks* 63 (4): 306–326.
Ouyang, M., and L. Duenas-Osorio. 2012. "Time-dependent resilience assessment and improvement of urban infrastructure systems." *Chaos Interdiscip. J. Nonlinear Sci.* 22 (3): 033122. https://doi.org/10.1063/1.4737204.
Ouyang, M., L. Duenas-Osorio, and X. Min. 2012. "A three-stage resilience analysis framework for urban infrastructure systems." *Struct. Saf.* 36–37: 23–31.
Pant, R., K. Barker, J. E. Ramirez-Marquez, and C. M. Rocco. 2014. "Stochastic measures of resilience and their application to container terminals." *Comput. Ind. Eng.* 70: 183–194. https://doi.org/10.1016/j.cie.2014.01.017.
Reed, D. A., K. C. Kapur, and R. D. Christie. 2009. "Methodology for assessing the resilience of networked infrastructure." *IEEE Syst. J.* 3 (2): 174–180. https://doi.org/10.1109/JSYST.2009.2017396.
Rocco, S., M. Claudio, J. E. Ramirez-Marquez, A. Salazar, E. Daniel, and E. Zio. 2010. "A flow importance measure with application to an italian transmission power system." *Int. J. Performability Eng.* 6 (1): 53–61.
Rodrigue, J. P., C. Comtois, and B. Slack. 2013. *The geography of transport systems*. Abingdon, UK: Routledge.
Rosato, V., S. Bologna, and F. Tiriticco. 2007. "Topological properties of high-voltage electrical transmission networks." *Electr. Power Syst. Res.* 77 (2): 99–105. https://doi.org/10.1016/j.epsr.2005.05.013.
RTE (Le Réseau de Transport d'Electricité). 2013. "French electricity transmission network 400-kV." Accessed January 2013. www.rte-france.com/uploads/media/CS4_2013.pdf.
Salmeron, J., and R. K. Wood. 2015. "The value of recovery transformers in protecting an electric transmission grid against attack." *IEEE Trans. Power Syst.* 30 (5): 2396–2403. https://doi.org/10.1109/TPWRS.2014.2360401.
Solé, R. V., M. Rosas-Casals, B. Corominas-Murtra, and S. Valverde. 2008. "Robustness of the European power grids under intentional attack." *Phys. Rev. E* 77 (2): 026102. https://doi.org/10.1103/PhysRevE.77.026102.
Sullivan, J. L., D. C. Novak, L. Aultman-Hall, and D. M. Scott. 2010. "Identifying critical road segments and measuring system-wide robustness in transportation networks with isolating links: A link-based capacity-reduction approach." *Transp. Res. Part A: Policy Pract.* 44 (5): 323–336.
TDM (Transportation Demand Management). 2013. "Online TDM encyclopedia." Accessed January 2, 2017. www.vtpi.org.
Vromans, M. J. C. M., R. Dekker, and L. G. Kroon. 2006. "Reliability and heterogeneity of railway services." *Eur. J. Oper. Res.* 172 (2): 647–665. https://doi.org/10.1016/j.ejor.2004.10.010.
Vugrin, E. D., and R. C. Camphouse. 2011. "Infrastructure resilience assessment through control design." *Int. J. Crit. Infrastruct.* 7 (3): 243–260. https://doi.org/10.1504/IJCIS.2011.042994.
Wang, S., L. Hong, M. Ouyang, J. Zhang, and X. Chen. 2013. "Vulnerability analysis of interdependent infrastructure systems under edge attack strategies." *Saf. Sci.* 51 (1): 328–337. https://doi.org/10.1016/j.ssci.2012.07.003.
Waters, N. 2006. "Network and nodal indices. Measures of complexity and redundancy: A review." In *Spatial dynamics, networks and modelling*, 16–33. Cheltenham, UK: Edward Elgar Publishing.
Wei, Y., C. Ji, F. Galvan, S. Couvillon, G. Orellana, and J. Momoh. 2016. "Non-stationary random process for large-scale failure and recovery of power distribution." *Appl. Math.* 7 (03): 233–249. https://doi.org/10.4236/am.2016.73022.
White House. 2013. *Presidential policy directive 21: Critical infrastructure security and resilience*. Washington, DC: Office of the Press Secretary.
Xu, N., S. D. Guikema, R. Davidson, L. Nozick, Z. Cagnan, and K. Vaziri. 2007. "Optimizing scheduling of post-earthquake electric power restoration tasks." *Earthquake Eng. Struct. Dyn.* 36 (2): 265–284.
Zhang, C., J. E. Ramirez-Marquez, and C. Rocco. 2011. "A new holistic method for reliability performance assessment and critical components detection in complex networks." *IIE Trans.* 43 (9): 661–675.
Zhang, X., E. Miller-Hooks, and K. Denny. 2015. "Assessing the role of network topology in transportation network resilience." *J. Transp. Geogr.* 46 (45): 35–45. https://doi.org/10.1016/j.jtrangeo.2015.05.006.
Zio, E., G. Sansavini, R. Maja, and G. Marchionni. 2008. "An analytical approach to the safety of road networks." *Int. J. Reliab. Qual. Saf. Eng.* 15 (1): 67–76. https://doi.org/10.1142/S0218539308002939.